Study on DC Voltage Control of Hybrid Active Power Filters

Xiao-Xi Cui, Chi-Seng Lam, Ning-Yi Dai, Wai-Hei Choi, Man-Chung Wong
Department of Electrical and Electronics Engineering
University of Macau
Macau, SAR, P. R. China
sunstarcxx@msn.com

Abstract—**This paper presents a DC voltage control analysis for hybrid active power filters (HAPF) under current-mode control scheme. Based on the analysis, it is clearly shown that adding the instantaneous DC voltage control signal as a reactive control parameter is more effective than adding the signal as an active control parameter for the DC voltage control. A control strategy is introduced to improve the performance of DC voltage control during start-up process. Finally, simulation results are given to verify the correctness of the DC voltage control analysis and illustrate the advantages of the control strategy for the start-up process.**

Keywords-hybrid acitve power filters; DC voltage control; start-up process

I. INTRODUCTION

Due to the proliferation and development of power electronics equipments (nonlinear loads) in utility power system, the power quality problems such as reactive power, current harmonics and neutral current in power system are deteriorated [1]–[2]. These power quality problems may affect the safety operation and increase the loss of the power grid and electrical equipments. In order to solve the power quality problems, power filters are widely used. Passive filter (PF) has been widely applied to suppress current harmonics and improve power factor due to its low cost and simplicity. However, it has some drawbacks such as resonance problems, low dynamic response, dependent filtering characteristics, etc. [3]–[4]. Active power filter (APF) can overcome the above mentioned drawbacks inherent in PF, but the initial and running costs of the APF are much higher than the PF [5]–[6], Therefore, it comes up with a hybrid active power filter (HAPF), which combines the advantages of PF and APF, and it is characterized by low cost and good performance [7]–[8].

For the conventional APF, when the APF works under current-mode control scheme, the DC voltage control is done by adding the dc voltage control signal to the compensation current as an active component. For the DC voltage control of HAPF, when the HAPF works under voltage-mode control, the DC voltage control is usually done by adding the dc voltage control signal as a reactive voltage component at the output voltage of inverter [9]–[10]. Up to now, there are seldom research works investigating the DC voltage control of a HAPF under current-mode control. Due to the fact that current-mode control is simple, easy to realize and less dependent on filter structure, analyzing DC voltage control under current-mode control is necessary. Moreover, if the HAPF DC voltage start-up process is done by conventional PI control, a long charging time and large overshoot may be as a consequence. In order to shorten the charging time and reduce the overshoot, a smooth start-up process is preferable, as the long charging time and large overshoot will affect the compensation performance and costs of the HAPF.

In this paper, the DC voltage control scheme of the HAPF under current-mode is studied and analyzed. Based on the analysis, it is found that adding the DC voltage control signal as a reactive component is more effective for control the DC voltage, compared with adding the DC signal as an active control parameter. To improve the performance of DC voltage control during the start-up process, a control strategy is introduced for getting a faster and smoother DC voltage control than the conventional PI control method. This paper is arranged into four main sections. In Section II, two DC voltage control methods of the HAPF are presented and analyzed under current-mode scheme, a start-up process with reducing the DC voltage control overshoot and charging time is introduced in Section III. Finally simulation results are shown to verify the DC voltage control scheme and all the analysis.

II. DC VOLTAGE CONTROL ANALYSIS UNDER CURRENT CONTROLLED HYBRID ACTIVE POWER FILTERS

A. Structure of current-mode control HAPF

A simplified HAPF structure is shown in Fig. 1. It consists of a coupling inductance L_c and capacitance C_c set and an inverter with a DC capacitance. u_s is the source voltage, u_L is the load voltage, u_{inv} is the output voltage of inverter, i_s is the source current, i_L is the load current, i_c is the compensation current.

978-1-4244-8756-1/11/$26.00 ©2011 IEEE

The following analyses are all based on fundamental frequency in which harmonic components are not considered. Consider the power of the source, load and HAPF, there is:

$$\begin{aligned} P_s &= P_L + P_{HAPF} \\ u_s i_{sp} &= u_L i_{Lp} + u_L i_{cp} \end{aligned} \tag{1}$$

where P_s, P_L and P_{HAPF} are the active power of the source, load and HAPF respectively, i_{sp}, i_{cp} and i_{Lp} are the active components of i_s, i_c and i_L. Since HAPF is constructed by passive part and active part, thus, the active power changing of HAPF ΔP_{HAPF} can be expressed as:

$$\Delta P_{HAPF} = \Delta P_{PF} + \Delta P_{inv} \tag{2}$$

In HAPF, the internal resistance of the passive part is usually small, which can be neglected, so $\Delta P_{PF} \cong 0$, and the changing active power can only deliver into the inverter for supporting the power losses of switching devices (IGBT) and the interchanging power of DC bus voltage. The active power changing of HAPF ΔP_{HAPF} can be rewritten as:

$$\Delta P_{HAPF} = \Delta P_{inv} = \Delta P_{dc} + \Delta P_{loss} \tag{3}$$

From (3), it can be shown that the change in active power of HAPF ΔP_{HAPF}, contributed by the sum of switching power losses ΔP_{loss}, and the active power change in DC-link ΔP_{dc}. ΔP_{loss} and ΔP_{dc} can also be expressed as:

$$\begin{aligned} \Delta P_{loss} &= u_L \Delta i_{cp\_loss} \\ \Delta P_{dc} &= u_L \Delta i_{cp\_dc} \end{aligned} \tag{4}$$

where Δi_{cp_loss} and Δi_{cp_dc} are the active changing currents for switching losses and DC bus voltage control respectively. According to (4), since u_L is constant, the active power change in DC-link ΔP_{dc}, only relates to the changing current Δi_{cp_dc}.

Since this current-mode control scheme is based on an ideal hysteresis PWM control, the hysteresis band is set zero and the inverter voltage can be expressed as:

$$\begin{cases} u_{inv} = u_{dc} & when \quad i_c^* - i_c > 0 \\ u_{inv} = -u_{dc} & when \quad i_c^* - i_c < 0 \end{cases} \tag{5}$$

where i_c^* is the instantaneous reference compensation current, i_c is the instantaneous compensation current. From (5), the instantaneous inverter output voltage u_{inv} can also be written as:

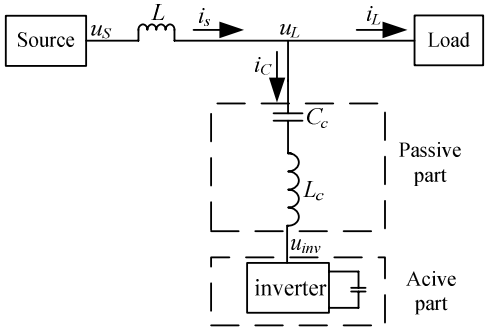

Figure 1. Simplified hybrid active power filter

$$u_{inv} = f(t)(i_c^* - i_c) \tag{6}$$

From (6), $f(t)$ is a nonlinear function and represents the relationship between u_{inv} and i_c^*-i_c. According to hysteresis PWM control scheme, u_{inv}=u_{dc} when i_c^*-i_c>0; u_{inv}=-u_{dc} when i_c^*-i_c<0, therefore it yields $f(t)$>0.

For the instantaneous compensation current i_c,

$$i_c = i_{cp} + i_{cq} \tag{7}$$

where i_{cp} and i_{cq} are the active and reactive component of i_c respectively. If the instantaneous terminal voltage is assumed as $U_L cos(\omega kT)$, the active component i_{cp} and reactive component i_{cq} can be expressed as $I_{cp} cos(\omega kT)$ and $I_{cq} sin(\omega kT)$. Thus, the instantaneous compensation current i_c at kT time can be rewritten as:

$$i_c = I_{cp} \cos(\omega kT) + I_{cq} \sin(\omega kT) \tag{8}$$

where $\omega = 2\pi f$ is the fundamental frequency, T is the sampling time, k is the discrete sequence with $k=0,1,2,3...n$.

B. Adding the DC voltage control signal as an active component

When the DC voltage control signal is added as an active component under current-mode control scheme, the control strategy can be shown in Fig. 2. From Fig. 2, C_2 and C_1^{-1} are the matrixes listed in section III. u_{dc} is the instantaneous DC voltage, u_{dc}^* is the instantaneous reference DC voltage, $\Delta\overline{i_{dc}}$ is the DC voltage control signal.

For adding the DC voltage control signal to the active part of i_c^*, i_c^* at next sampling time $(k+1)T$ can be written as:

$$i_c^* = (I_{cp} + \Delta\overline{i_{dc}}) \cos(\omega(k+1)T) + I_{cq} \sin(\omega(k+1)T) \tag{9}$$

Substituting (9) and (8) into (6), the instantaneous output voltage of inverter u_{inv} becomes:

$$u_{inv} = f(t)[\Delta\overline{i_{dc}} \cos(\omega(k+1)T) + H] \tag{10}$$

where H represents those parameters that are not related with $\Delta\overline{i_{dc}}$ and $H=I_{cp}[cos(\omega(k+1)T)-cos(\omega kT)]+I_{cq}[sin(\omega(k+1)T)-cos(\omega kT)]$.

According to (10) and (8), the instantaneous apparent power of inverter S_{inv} is:

$$\begin{aligned} S_{inv} &= u_{inv} i_c \\ &= f(t)[\Delta\overline{i_{dc}} \cos(\omega(k+1)T) + H] \cdot \\ &\quad [I_{cp} \cos(\omega kT) + I_{cq} \sin(\omega kT)] \end{aligned} \tag{11}$$

The instantaneous changing apparent power caused by adding $\Delta\overline{i_{dc}}$ is:

$$\begin{aligned} \Delta S_{dc} = &\frac{1}{2} f(t) \Delta\overline{i_{dc}} I_{cp} \cos((2k+1)\omega T) + \frac{1}{2} f(t) \Delta\overline{i_{dc}} I_{cp} \cos(\omega T) \\ &+ \frac{1}{2} f(t) \Delta\overline{i_{dc}} I_{cq} \sin((2k+1)\omega T) - \frac{1}{2} f(t) \Delta\overline{i_{dc}} I_{cq} \sin(\omega T) \end{aligned} \tag{12}$$

Neglect the instantaneous apparent power which is in cycle, the instantaneous changing active power caused by adding Δi_{dc} is:

$$\Delta P_{dc} = \frac{1}{2} f(t)\Delta\overline{i_{dc}} I_{cp}\cos(\omega T) - \frac{1}{2} f(t)\Delta\overline{i_{dc}} I_{cq}\sin(\omega T) \quad (13)$$

Substitutes (13) into (4), the active changing current Δi_{cp_dc} for DC bus voltage control can be written as:

$$\Delta i_{cp\_dc} = \frac{\frac{1}{2} f(t)\Delta\overline{i_{dc}} I_{cp}\cos(\omega T) - \frac{1}{2} f(t)\Delta\overline{i_{dc}} I_{cq}\sin(\omega T)}{u_L} \quad (14)$$

From (13) and (14), ω and T are constants, T is assumed close to zero due to high sampling frequency ($T \cong 0$), therefore, $cos(\omega T) \cong 1$ $sin(\omega T) \cong 0$. Both the active power P_{dc} and the active current component Δi_{cp_dc} of DC-link are functions of Δi_{dc} and I_{cp}. Moreover, since I_{cp} is dependent on the inverter characteristic, so that Δi_{dc} is the only control signal for DC bus voltage control. Therefore, adding the DC voltage control signal as an instantaneous active component is possible to control the DC voltage when the HAPF works on current-mode.

C. Adding the DC voltage control signal as a reactive component

When the DC voltage control signal is added as an instantaneous reactive component under current-mode control scheme, as shown in Fig. 3. From Fig. 3, C_2 and C_1^{-1} are the same matrixes as shown in Fig. 2. This current-mode control scheme is also based on hysteresis PWM control. Therefore, u_{inv} and i_c can still be expressed as (6) and (8). In this part, the DC voltage control signal is added to the instantaneous reactive part of i_c^*, which can be expressed as:

$$i_c^* = I_{cp}\cos(\omega(k+1)T) + (I_{cq} + \Delta\overline{i_{dc}})\sin(\omega(k+1)T) \quad (15)$$

Substituting (15) and (8) into (6), the instantaneous output voltage of inverter u_{inv} can be expressed as:

$$u_{inv} = f(t)[\Delta\overline{i_{dc}}\sin(\omega(k+1)T) + H] \quad (16)$$

where H represents those parameters that are not related with Δi_{dc}, and has the same expression as shown in (10).

According to (16) and (8), the instantaneous apparent power of inverter S_{inv} is:

$$\begin{aligned} S_{inv} &= u_{inv} i_c \\ &= f(t)[\Delta\overline{i_{dc}}\sin(\omega(k+1)T) + H]\cdot \\ &\quad [I_{cp}\cos(\omega kT) + I_{cq}\sin(\omega kT)] \end{aligned} \quad (17)$$

The instantaneous changing apparent power caused by adding Δi_{dc} is:

$$\begin{aligned} \Delta S_{dc} = &\frac{1}{2} f(t)\Delta\overline{i_{dc}} I_{cp}\sin((2k+1)\omega T) + \frac{1}{2} f(t)\Delta\overline{i_{dc}} I_{cp}\sin(\omega T) \\ &+ \frac{1}{2} f(t)\Delta\overline{i_{dc}} I_{cq}\cos((2k+1)\omega T) + \frac{1}{2} f(t)\Delta\overline{i_{dc}} I_{cq}\cos(\omega T) \end{aligned} \quad (18)$$

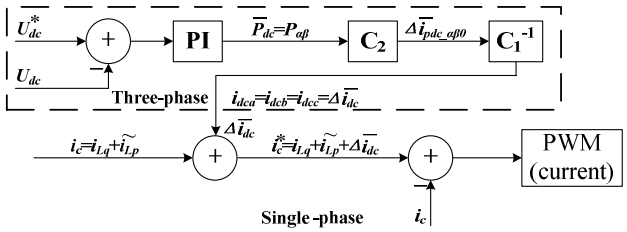

Figure 2. Current-mode control scheme with DC voltage control signal is added as an instantaneous active component

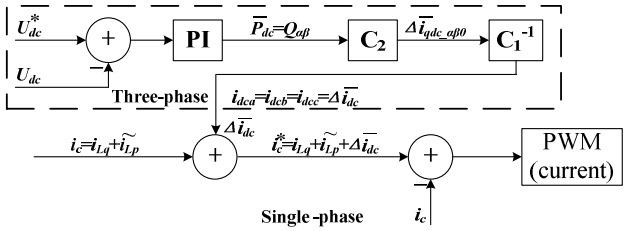

Figure 3. Current-mode control scheme with DC voltage control signal is added as an instantaneous reactive component

Neglect the instantaneous apparent power which is in cycle, the instantaneous changing active power caused by adding Δi_{dc} is:

$$\Delta P_{dc} = \frac{1}{2} f(t)\Delta\overline{i_{dc}} I_{cq}\cos(\omega T) + \frac{1}{2} f(t)\Delta\overline{i_{dc}} I_{cp}\sin(\omega T) \quad (19)$$

Substitute (19) into (4), the active changing currents Δi_{cp_dc} for control DC bus voltage can be written as:

$$\Delta i_{cp\_dc} = \frac{\frac{1}{2} f(t)\Delta\overline{i_{dc}} I_{cq}\cos(\omega T) + \frac{1}{2} f(t)\Delta\overline{i_{dc}} I_{cp}\sin(\omega T)}{u_L} \quad (20)$$

Similar as part B, ω and T are constants, T is very small ($T \cong 0$). I_{cq} is dependent on the load characteristic. It can also be deduced that the DC voltage of HAPF can only be controlled by Δi_{dc}. Therefore, adding the DC voltage control signal as an instantaneous reactive component is possible to control the DC voltage when the HAPF works on current-mode.

D. Comparison

Table I summarizes the analysis results of two DC voltage control strategies. From Table I, when the DC voltage control signal Δi_{dc} is the same for the two DC voltage control strategies, adding the DC voltage control signal as an instantaneous reactive component is more effective than adding the signal as an active component due to the reactive current I_{cq} is always larger than the active current I_{cp} in HAPF. This is because HAPF aims at compensating reactive power and current harmonics. In order to have an effective DC voltage control, DC voltage control signal should be added as an instantaneous reactive component to the reference compensating current i_c^*.

III. CONTROL OF THE HYBRID ACTIVE POWER FILTERS WITH DC VOLTAGE AND START-UP CONSIDERATION

The three-phase four-wire structure of the HAPF and its compensation control algorithm are shown in Fig. 4 and Fig. 5 respectively. From Fig. 5, P_{dc} is the DC voltage control signal. i_a, i_b and i_c are the three-phase load currents, U_a, U_b and U_c are the three-phase source voltages. U_{dc}^* is the DC capacitor reference voltage and U_{dc} is the DC capacitor voltage. C_1 shown in (21) is a matrix that transforms *abc* coordinate into $\alpha\beta 0$ coordinate. C_1^{-1} shown in (22) is the inverse matrix of C_1. C_2 shown in (23) is a matrix to transform the power into current in $\alpha\beta 0$ coordinate. According to (23), the currents in $\alpha\beta 0$ coordinate can be calculated as in (24). C_3 shown in (25) is the matrix to calculate the fundamental active current in $\alpha\beta 0$ coordinate. From (25), the fundamental active currents in $\alpha\beta 0$ coordinate can be calculated by (26). T_1 is a square sum process.

$$C_1 = \sqrt{\frac{2}{3}}\begin{bmatrix} \frac{1}{\sqrt{2}} & \frac{1}{\sqrt{2}} & \frac{1}{\sqrt{2}} \\ 1 & -\frac{1}{2} & -\frac{1}{2} \\ 0 & \frac{\sqrt{3}}{2} & \frac{\sqrt{3}}{2} \end{bmatrix} \tag{21}$$

$$C_1^{-1} = \sqrt{\frac{2}{3}}\begin{bmatrix} 1 & 0 & \frac{1}{\sqrt{2}} \\ -\frac{1}{2} & \frac{\sqrt{3}}{2} & \frac{1}{\sqrt{2}} \\ -\frac{1}{2} & -\frac{\sqrt{3}}{2} & \frac{1}{\sqrt{2}} \end{bmatrix} \tag{22}$$

$$C_2 = \frac{1}{u_0^2 u_{\alpha\beta}^2}\begin{bmatrix} u_{\alpha\beta}^2 & 0 & 0 \\ 0 & u_0 u_\alpha & -u_0 u\beta \\ 0 & u_0 u\beta & u_0 u_\alpha \end{bmatrix} \tag{23}$$

$$\begin{bmatrix} i_0 \\ i_\alpha \\ i_\beta \end{bmatrix} = C_2 \begin{bmatrix} p_0 \\ p_{\alpha\beta} \\ q_{\alpha\beta} \end{bmatrix} \tag{24}$$

TABLE I. ANALYSIS RESULTS OF TWO DC VOLTAGE CONTROL STRATEGIES BASED ON CURRENT-MODE

DC control signal	Controllable signal	Controlled active power	Controlled active current
active current	i_{Lfp}	$\frac{1}{2} f(t)\Delta\overline{i_{dc}} I_{cp}$	$\frac{\frac{1}{2} f(t)\Delta\overline{i_{dc}} I_{cp}}{u_L}$
reactive current	i_{Lfq}	$\frac{1}{2} f(t)\Delta\overline{i_{dc}} I_{cq}$	$\frac{\frac{1}{2} f(t)\Delta\overline{i_{dc}} I_{cq}}{u_L}$

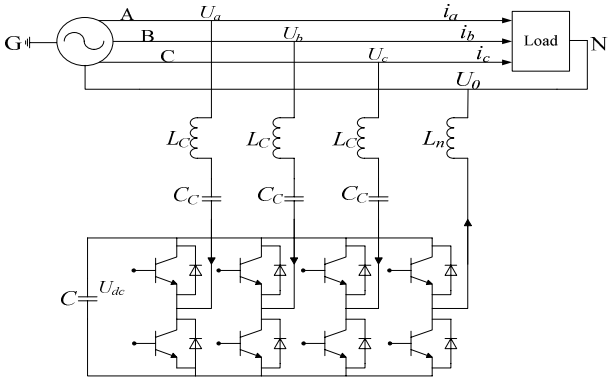

Figure 4. Structure of three-phase four-wire HAPF

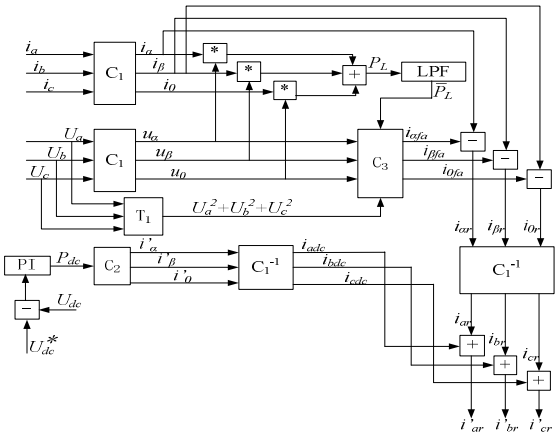

Figure 5. Compensation control algorithm of HAPF

$$C_3 = \left(\frac{1}{u_\alpha^2 + u_\beta^2 + u_0^2}\right)\begin{bmatrix} \overline{P}_L & \overline{P}_L & \overline{P}_L \end{bmatrix} \tag{25}$$

$$\begin{bmatrix} i_{\alpha fa} \\ i_{\beta fa} \\ i_{0\,fa} \end{bmatrix} = C_3 \begin{bmatrix} u_\alpha \\ u_\beta \\ u_0 \end{bmatrix} \tag{26}$$

To calculate u_α, u_β, u_0 and $u_{\alpha\beta}$ are shown in [11]. From (24), when the DC voltage is added as an instantaneous active component, $p_{\alpha\beta}$ equals to the DC voltage control signal, P_{dc} and p_0 $q_{\alpha\beta}$ equal to zero. When the DC voltage control signal is added as an instantaneous reactive component, $q_{\alpha\beta}$ equal to the DC voltage control signal P_{dc} and p_0, $p_{\alpha\beta}$ equal to zero.

From Fig. 5, the DC voltage is controlled by a PI controller. If the HAPF connects to the system with initial DC voltage equal to zero, a long settling time and large overshoot may occur due to the characteristics of PI control. When there is no special control strategy during start-up process, the error between U_{dc}^* and U_{dc} is the maximum at the beginning, that causes a large error accumulation before the voltage reaches the reference voltage. Due to the large error accumulation, the PI controller will cause a large overshoot and long settling time. To avoid those drawbacks, a control strategy for start-up

process is introduced, in which the block diagram of the start-up process is shown in Fig. 6.

During the start-up process, all the IGBTs are forced to turn off to let the anti-parallel diodes act as a three-phase uncontrollable rectifier. Under the rectification circuit, the DC capacitor will be quickly charged. Once the DC voltage reaches its reference voltage value, the compensation with DC voltage control algorithm starts, therefore, the initial value of U_{dc} is close to U_{dc}^*, the large overshoot and long settling time can be avoided.

IV. SIMULATION RESULTS

Simulations are done by PSCAD. The simulation load model is shown in Fig. 7, and the system parameters of HAPF are summarized in Table II, L_n is the neutral line inductance and U_{dc}^* is the reference DC voltage.

Fig. 8 (a) shows the charging process of the DC bus voltage by adding the control signal as an active component, from Fig. 8 (a), during 0 to 0.2s the HAPF disconnects with the power system. At 0.2s the HAPF is connected to operate with DC voltage PI control and compensation control operation. At 1.25s the DC voltage is charged to the reference voltage, it takes 1.05s after the HAPF connects to the power system. At 3.9s the DC bus voltage operates in steady state, it takes 2.65s after the DC bus voltage charged to the reference voltage. During this voltage charging process, the maximum voltage overshoot is 33.3V. Fig. 8 (b) shows the charging control process of the DC bus voltage by adding the control signal as a reactive component when the HAPF works on current-mode control scheme. From Fig. 8 (b), during 0 to 0.2s the HAPF disconnects with the power system. At 0.2s the HAPF is connected to the power system with DC voltage PI control and compensation control operation. At 0.36s the DC voltage is charged to the reference voltage, it takes 0.16s after the HAPF is connected to the power system. At 1.5s the DC voltage goes to a steady state, it takes 1.14s after the DC voltage is charged to the reference voltage. During this voltage charging process, the maximum voltage overshoot is 6.3V. Comparing the charging time, settling time and overshoot of the two control strategies, the results are summarized in Table III. From Table III, adding the DC voltage control signal as a reactive component is more effective for the DC voltage control than that of adding as an active component.

To improve the performance of DC voltage control when the DC voltage is controlled by the reactive component, a start-up control strategy is added, the simulation result is shown in Fig. 9. From Fig. 9, before 0.2s the HAPF disconnects with the system, at 0.2s the HAPF is connected to the system and all the IGBTs are forced to turn off to become a rectification circuit. At 0.36s the DC voltage is charged to the reference voltage. In order to clearly show the DC voltage control results, the reference voltage will be hold until 0.6s. At 0.6s the DC voltage PI control and compensation control will be operated. Compared with the DC voltage control under reactive component but without start-up process, the results are summarized in Table IV. From Table IV, it is clearly shown that the advantages of the additional start-up control strategy.

Fig. 10 shows the three-phase source current and neutral current before and after compensation, the compensation results are summarized in Table V. All the compensation results are satisfied with IEC and IEEE standards.

TABLE II. HAPF SYSTEM PARAMETERS FOR SIMULATION

U_S	C_c	L_c	L_n
220 *V*	81 *uf*	0.005 *h*	0.002 *h*
R_L	C_L	L_L	U^*_{dc}
26 *omh*	200 *uf*	0.03 *h*	30 *V*

TABLE III. COMPARISON RESULTS BETWEEN DIFFERENT DC CONTROL COMPONENTS

DC control component	Charging time	Settling time	Maximum Overshoot
Active component	1.05 *s*	2.65 *s*	33.3 *V*
Reactive component	0.16 *s*	1.14 *s*	6.3 *V*

TABLE IV. DC VOLTAGE CONTROL RESULTS WITH AND WITHOUT START-UP PROCESS

DC control component	With start-up process	Charging time	Settling time	Maximum Overshoot
Reactive component	NO	0.16 *s*	1.14 *s*	6.3 *V*
Reactive component	YES	0.16 *s*	0 *s*	0 *V*

TABLE V. SIMULATION RESULTS FOR HAPF

Before compensation		After compensation	
Power factor	THD	Power factor	THD
0.83	29.48	0.99	3.57

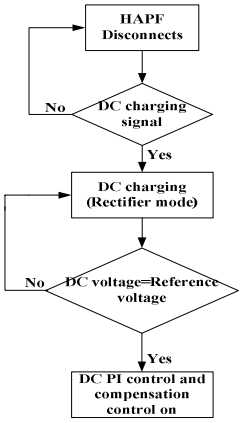

Figure 6. Block diagram of start-up process

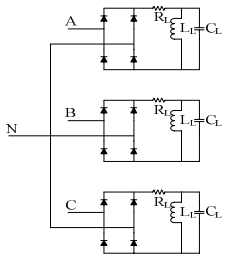

Figure 7. Load model for simulation

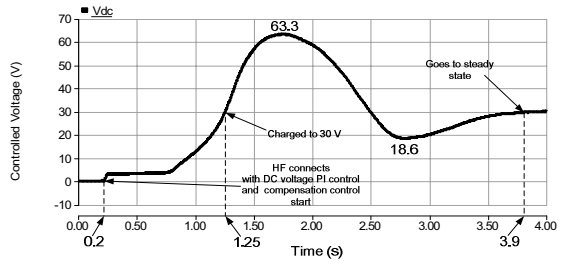

(a) DC voltage control (acitve component)

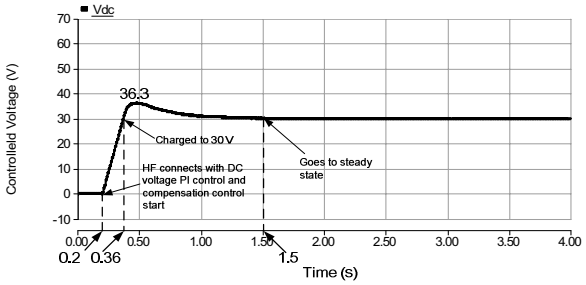

(b) DC voltage control (reacitve component)

Figure 8. DC voltage control with PI controller

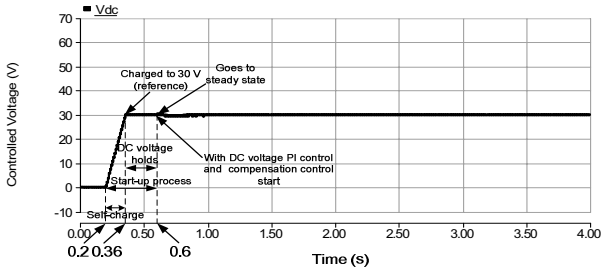

Figure 9. DC voltage control with start-up control and PI controller

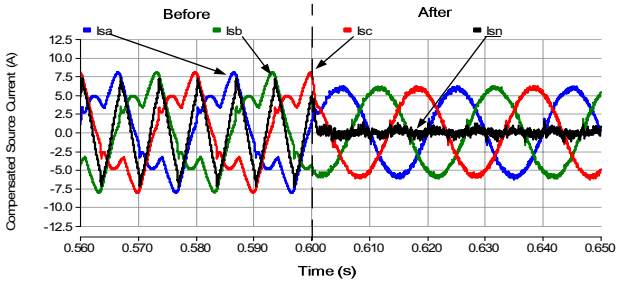

Figure 10. Source and netural currents before and after compensation

V. CONCULATIONS

This paper analyzes the DC voltage control when the HAPF is operating under current-mode control scheme. After the theoretical analysis and simulation results, adding the DC voltage control signal to the reactive part of the reference compensating current is concluded to be more effective than adding the signal to the active part. In order to reduce the overshoot and long settling time for the PI control during the start-up process, a start-up control strategy is introduced. Finally, simulation results are given to verify all the DC voltage control analysis and to show the advantages of the presented control strategy over the PI control during the start-up process.

Acknowledgment

The authors would like to thank the Science and Technology Development Fund, Macao SAR Government and University of Macau for their financial supports.

REFRERNCES

[1] S. M. Williams, G.T.Brownfield, and J. W. Duffus, "Harmonic propagation on an electric distribution system: field measurements compared with computer simulation," IEEE Trans. on *Power Delivery*, vol. 8, no. 2, pp.547-552, April 1993.

[2] S. Lee and C. Wu, "On-Line Reactive Power Compensation Schemes for Unbalanced Three Phase Four Wire Distribution Feeders," IEEE Trans. on *Power Delivery*, vol. 8, no. 4, pp. 1958-1965, October 1994.

[3] H. Fujita, T. Yamasaki, H. Akagi, "A hybrid active filters for damping of harmonic resonce in industrial power system," IEEE Trans. on *Power Electrics*, vol 15, issue. 2, pp. 215-222, 2000..

[4] F.Z. Peng, H. Akagi, A. Nanbe, "A new approach to harmonic compensation in power systems- A combined system of shunt passive and series active filters," IEEE Trans. on *Ind. Appt*, vol. 26, pp. 983-990, november 1990.

[5] D. Rivas, L. Moran, J. W. Dixon, J. R. Espinoza, "Improving passive filter compensation performance with acitve techniques," IEEE Trans. on *Industrial Electronics*, vol. 50, pp. 161-170, Febrary 2003.

[6] B. Singh, K. Al-Haddad, A. Chandra, "A review of active filters for power quality improvement," IEEE Trans. on *Industrial Electronics*, vol. 46, no. 5, pp. 960-971, Octomber 1999.

[7] H. –L.Jou, J. –C. Wu, K. –D. Wu, "Parallel operation of passive power filter and hybrid power filter for harmonic suppression," IEEE Trans. on *Generation, Transmission and Distribution*, Vol. 148, pp. 8-14, 2001.

[8] M. Rastogi, N. Mohan, A.-A Edris, "Hybrid-active filteing of harmonic currents in power systems," IEEE Trans. on *Power Delivery*, vol. 10, Issue. 4, pp.1994-2000, 1995.

[9] H. Akagi, "Active harmonic filters," Proceeding of the IEEE, vol. 93, issue. 12, pp. 2128-2141, 2005.

[10] R. Inzunza, H. Akagi, "A 6.6-kV transformerless shunt hybrid active filter for installation on a power distribution system," IEEE Trans. on *Power Electronics*, vol. 20, pp. 893-900, July 2005.

[11] Herrera, R.S, Salmeron, P, "Present point of view about the instantaneous reactive power theory," IEEE Trans. on *Power Electronics*, vol. 2, issue. 5, pp. 484-495, 2009.